Recovery of the ionic liquids [C_2mim][OAc] or [C_2mim][SCN] by distillation from their binary mixtures with methanol or ethanol

Marta K. Wojtczuk, Nuria Caeiro, Héctor Rodríguez, Eva Rodil* and Ana Soto

CRETUS Institute, Department of Chemical Engineering, Universidade de Santiago de Compostela, E-15782, Santiago de Compostela, Spain

* Corresponding author. E-mail address: eva.rodil@usc.es

Abstract

The ionic liquids 1-ethyl-3-methyl-imidazolium acetate ([C_2mim][OAc]) and 1-ethyl-3-methylimidazolium thiocyanate ([C_2mim][SCN]) have been proposed to improve many processes from the point of view of efficiency and/or sustainability. In a number of those proposals, mixtures of these ionic liquids with alcohols are generated. On the assumption of easy separation of the volatile alcohol and the totally non-volatile ionic liquid by distillation, little attention has been paid to the recovery of the ionic liquid to date. However, this is a critical step to transform a process tested at laboratory level into an industrial reality. To analyse the viability of using distillation to recover the above mentioned ionic liquids from their mixtures with methanol or ethanol, in this work the isobaric vapour-liquid equilibria of the corresponding binary systems at pressures of 101.32, 50, and 25 kPa were determined. Several physical and derived properties were also determined for the studied systems at 298.15 K and atmospheric pressure. The simulation of a flash unit, using the correlation of the experimental data with the NRTL model, was carried out with Aspen Plus at different temperatures and pressures. High ionic liquid purities were obtained in the case of the systems comprising [C_2mim][SCN], which could be satisfactorily recovered at moderate vacuum. However, in the case of systems involving [C_2mim][OAc], the recovery was limited by the relatively low degradation temperature of this ionic liquid.

Keywords: Ionic liquid, solvent recovery, vapour-liquid equilibrium, process simulation, flash distillation.

1. Introduction

Ionic liquids (ILs) have received increasing attention from academia and industry over the last couple of decades, due to their attractive set of properties. For a good number of compounds of the IL family, this set typically includes properties such as negligible volatility, non-flammability, good thermal and chemical stabilities, and great solvation ability [1]. Moreover, the physical, chemical and biological properties of ILs can be tuned to a significant extent by judicious selection and functionalisation of the constituent ions [1, 2], tailoring them for specific applications. In spite of these appealing characteristics of ILs, the number of industrial applications involving these substances as neoteric solvents [3] can be considered still rather limited, in particular in the context of chemical processes. A critical aspect to develop competitive chemical processes using ILs is the efficient regeneration and recycling of the latter [4], thus contributing to the reduction of environmental impacts and to the improvement of the economy of the process. Given the negligible vapour pressure of ILs, their recovery from fluid mixtures where they are combined with volatile solvents has often been assumed as easy, via evaporation or distillation techniques. Considering the virtually infinite relative volatility of conventional molecular solvents and ILs, the unit operation of choice to carry out the recovery of the ILs in a scaled-up continuous process would be flash distillation (since regular rectification would lead to unrealistic high temperatures in the reboiler due to the negligible vapour pressure of the IL). For the suitable design of units for the performance of flash distillation (or any other kind of distillation technique), knowledge of the vapour-liquid equilibrium (VLE) of the fluid feed system is needed.

Steady-state simulation is a powerful tool in the chemical industry, not only to design a plant or a process, but also to optimise the conditions that enable more cost- and production-efficient, less energy-demanding, and less wasteful processes. However, the utilisation of reliable data with the corresponding uncertainties, the selection of an appropriate model and method of estimation of parameters, and the assessment of the simulation results are key factors in obtaining trustworthy results [5]. From a perspective of IL recovery by distillation, knowledge of the VLE is necessary for getting valuable information with the simulation software. Although simulation can be a decisive link between the experimental laboratory data and the industrial application, the number of research articles that consider this approach for processes involving recovery of ILs by distillation is still very low. Jongmans et al. [6] analysed the viability of using 1-butyl-4-

methylpyridinium tetrafluoroborate as entrainer in extractive distillation to separate the mixture ethylbenzene/styrene. One or two flash units, stripping with a hot gas (nitrogen or ethylbenzene), supercritical extraction, distillation by adding a co-solvent, and evaporation were different approaches investigated for solvent regeneration. The NRTL thermodynamic model was used, where the corresponding binary interaction parameters of compound pairs comprising the IL were obtained from experimental data of activity coefficients at infinite dilution. Evaporation using very low pressures and stripping with ethylbenzene were found to be the most promising alternatives. Ferro and co-workers [7-11] used COSMO-based simulations for the conceptual design of different processes to carry out the separation of mixtures of aromatic and aliphatic hydrocarbons. The authors found that, for naphtha of low aromatic content, similar separation efficiencies to liquid-liquid extraction were achieved by extractive distillation, requiring a lower solvent-to-feed ratio but higher energy consumption. Regarding naphtha with high aromatic content, extractive distillation performed better, with a significant reduction of the energy requirements [11]. (These findings are in line with the preferred separation techniques described by Weissermel et al. as a function of the aromatic content of the feed stream to be treated [12].) Flash units were systematically proposed for the recovery of the IL. Configurations with one to three flash distillation units were tested, and the one with three units was selected as the best in terms of the efficiency, although it also implied the highest energy requirements [10]. Kulajanpeng et al. [13] proposed a systematic methodology for the screening of ILs as entrainers in water/alcohol extractive distillation. These authors also proposed the recovery of the IL by means of a flash unit, followed by a stripper using air as stripping agent. Using the NRTL model (with the binary interaction parameters obtained from experimental VLE data), the authors were able to show that all the tested ILs were able to break the azeotrope. However, their simulation work rendered the separation of water/ethanol with 1-ethyl-3-methylimidazolium acetate as unfeasible, as a result of the extremely low operating pressure required to recover the IL due to its relatively low degradation temperature. A similar problem was found by Chen et al. [14] when they simulated the extractive distillation of the mixture water/isopropanol with the same IL. Finally, the UNIFAC-Lei model was used by Zhu et al. [15] to simulate the extractive distillation of the ethylacetate/ethanol mixture with four ILs tested as entrainers. As previously proposed by Kulajanpeng et al. [13], a flash unit followed by a stripper with air was selected as the method for IL recovery. The optimal design parameters were verified by economic evaluation.

In this work, we will follow an approach combining the rigorous experimental determination of VLE data and the subsequent simulation of a flash unit with a process simulation software, to explore the feasibility and optimal conditions of the recovery of two different ILs from their mixtures with an alcohol (either methanol or ethanol). The two ILs selected were 1-ethyl-3-methylimidazolium acetate ([C_2mim][OAc]) and 1-ethyl-3-methylimidazolium thiocyanate ([C_2mim][SCN]), which have been suggested in the literature as solvents in liquid-liquid extraction or as entrainers in extractive distillation for the separation of mixtures ester/alcohol [16-18], ketone/alcohol [19], or hydrocarbon/alcohol [20, 21] – the alcohol being either methanol or ethanol. Also, [C_2mim][OAc] is known to be an archetypical IL for the dissolution of lignocellulosic biomass, and in this context we have shown the potential of alcohols as cosolvents reducing the viscosity and tuning the capacity of this IL in the dissolution of lignocellulosic biopolymers, or as antisolvents for the regeneration of these biopolymers from the IL solution [22, 23]. In spite of this rather elevated number of prospective applications where mixtures of these ILs and alcohols appear, unfortunately no attention has been paid to the equilibrium data required to design the step of regeneration of the IL by vaporisation of the alcohols, nor to the significant energy penalty that it could entail. The integration of this regeneration step is crucial for the adequate assessment of the feasibility and viability of the IL-based processes in the potential applications considered. The present work aims to bring some light in this regard, specifically by determining the isobaric VLE data of the binary systems IL + alcohol at the absolutes pressures of 101.32, 50, and 25 kPa; followed by their utilisation in the production of reliable information of the separation processes by simulation with the Aspen Plus process simulation software. Particular attention will be devoted to the optimal conditions and energy requirements.

2. Experimental

2.1. Chemicals

Methanol and ethanol were supplied by Panreac with nominal purity of 99.8 % in both cases, and they were used as received. The ILs [C_2mim][OAc] (CAS number: 143314-17-4) and [C_2mim][SCN] (CAS number: 331717-63-6) were purchased from Iolitec with nominal purities >95 % and >98 %, respectively. To avoid the potential influence of the water content of the hygroscopic ILs in the results [24], they were dried under high vacuum (absolute pressure <1 Pa) with stirring at moderate temperature (ca.

338 K), for no less than 48 h. The final water contents of the dried batches, measured in a Metrohm 899 coulometer by the Karl-Fischer titration method, were 0.0012 and 0.0006 in mass fraction for [C_2mim][OAc] and [C_2mim][SCN], respectively. The absence of relevant levels of other impurities as well as the preservation of the chemical identities of the ILs after the drying treatment were assessed by ^{1}H and ^{13}C NMR spectroscopy, and the corresponding spectra are shown in Figures S1 to S4 in the Supplementary Material.

Several physical properties, namely density, refractive index, and the normal boiling temperature, were measured (as described in section 2.2) for the samples of the compounds used in this work. The corresponding values are listed in Table 1, where a good agreement with data from the literature [25-27] can be observed.

Table 1. Water mass fraction (w_{H2O}), density (ρ) and refractive index (n_D) at 298.15 K and atmospheric pressure, and normal boiling temperature (T_b) precisely at 101.32 kPa, experimentally measured in this work ("exp.") and taken from the literature ("lit.") [25-27], for the compounds involved in the studied systems. (No T_b is reported for the ionic liquids, as they undergo thermal decomposition upon heating before boiling.) [a]

Compound	w_{H2O}	ρ / g·cm^{-3}		n_D		T_b / K	
	exp.	exp.	lit.	exp.	lit.	exp.	lit.
Methanol	n.m.[b]	0.7868	0.78637	1.32660	1.32652	337.80	337.696
Ethanol	0.0005	0.7846	0.78493	1.35972	1.35941	351.48	351.443
[C_2mim][OAc]	0.0012	1.0990	1.09989	1.50069	1.5005	-	-
[C_2mim][SCN]	0.0006	1.1151	1.11170	1.55065	1.55064	-	-

[a] Uncertainties for determination of densities: $u(T)$ = 0.1 K, $u(P)$= 5 kPa, $u(\rho)$ = 0.0001 g/cm^3. Uncertainties for determination of refractive indices: $u(T)$ = 0.02 K, $u(P)$= 5 kPa, $u(n_D)$ = 0.00004. Uncertainties for determination of boiling temperatures: $u(P)$= 0.005 kPa, $u(T_b)$ = 0.05K
[b] n.m.: not measured.

2.2. Vapour-liquid equilibrium

Isobaric VLE data for the binary systems IL + alcohol were obtained in a Fischer Labor und Verfahrenstechnik Labodest 602 distillation apparatus that recycles both the liquid and vapour phases. This still is equipped with a Fischer digital manometer and an ASL F250 Mk II precision thermometer operating with a wired PT100 PRT probe. Distillation was carried out at 25 and 50 kPa with the help of a vacuum pump system, and at 101.32 kPa under inert argon atmosphere. The compositions of the liquid phases (in all cases) and vapour phases (just occasionally, to check that they corresponded to pure alcohol, due to the non-volatile character of the IL) at equilibrium were determined using the density measurement as analysis method. For such purpose, samples of IL + alcohol of known composition, covering the entire composition range, were prepared by weight

using a Mettler Toledo XPE205 analytical balance. The densities of all samples were measured in an Anton Paar DSA 48 density meter with internal control of temperature and automatic correction of the viscosity influence on the density. The characterisation of these samples was completed with the measurement of the speed of sound through them (performed simultaneously with the same apparatus) and their refractive indices. The latter were measured in an ATAGO RX-5000 refractometer connected to a HetoTherm thermostat to keep the temperature constant. At least two measurements of each property were performed at 298.15 K, ensuring that they were repeatable within the nominal uncertainties (0.0001 g/cm^3 for density, and 0.00004 for refractive index), and the average value was recorded.

2.3. Process simulation

Simulations were performed with the commercial software Aspen Plus v.9. ILs were created as user-defined components by specifying their molecular weights and critical properties (critical temperature, critical pressure, critical molar volume, and critical compressibility factor), that were taken from the literature [28]. It is worth mentioning that ILs typically decompose, in usual pressure ranges, at much lower temperatures than the ones corresponding to the critical points, so their critical property values are actually estimated rather than experimentally measured. The definition of these components was completed with vapour pressure and heat capacity correlation parameters found for these ILs in the literature [14, 29, 30]. All these parameters are presented in the Supplementary Material (Table S1). The NRTL model [31] was selected as the thermodynamic model to describe the non-ideality of the liquid phase. Its corresponding interaction parameters were obtained from the correlation of the experimental VLE data generated in this work.

Taking into account the negligible volatility of ILs, a flash unit was selected for the IL recovery from its mixtures with alcohol (Fig. 1). The feed stream was defined as 100 kmol/h of a mixture of IL + alcohol with a 0.20 mole fraction of IL, at 298.15 K and 101.32 kPa. The operating pressure of the flash tank was set to 101.32, 75, 50, 25, and 5 kPa. The required energy was supplied at two points: first, by means of a heater placed before the flash tank, allowing energy integration from product streams exiting the tank; and second, directly in the flash unit to reach the desired operation temperature. All the simulation runs were carried out considering that the temperatures should be kept below the reported decomposition temperatures of the ILs [22, 32, 33]. Thus, 423 K was set as

the operation temperature upper limit in the case of [C2mim][OAc], and 513 K in the case of [C2mim][SCN].

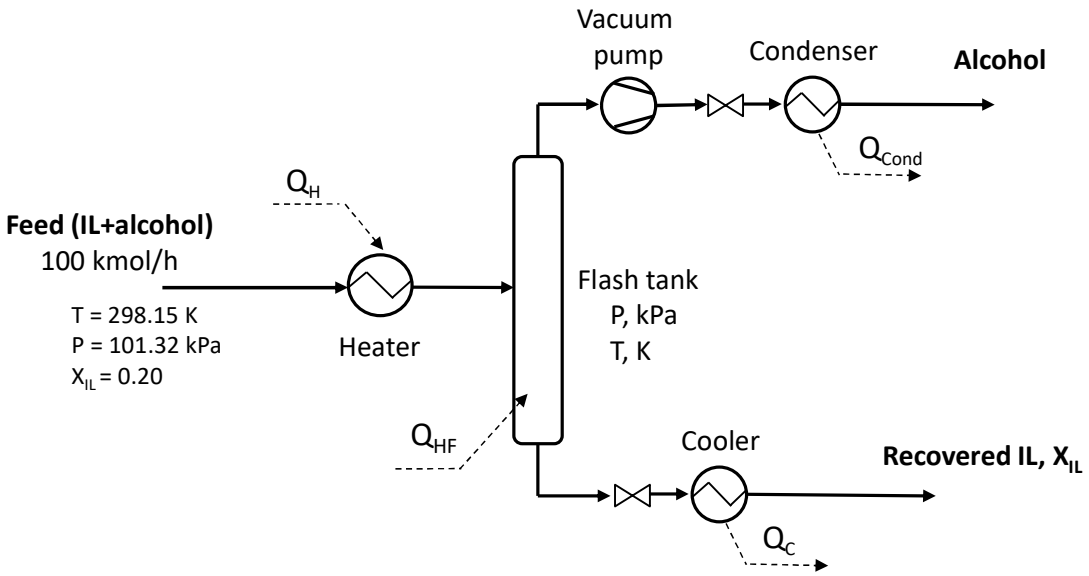

Fig. 1. Process flowsheet scheme and stream conditions for simulation of the IL recovery in Aspen Plus.

3. Results and discussion

3.1. Physical properties

Density (ρ), speed of sound (u), and refractive index (n_D), at 298.15 K and atmospheric pressure, are reported in Table 2 for the binary systems methanol + [C2mim][SCN] and ethanol + [C2mim][SCN] throughout the entire composition ranges. Since the utilisation of excess properties and changes of property by mixing typically enhances the degree of precision of compositional analyses based on physical properties, the excess molar volumes (V^E) were calculated from the experimental density values as follows:

$$V^E = \frac{x_1 \cdot M_1 + x_2 \cdot M_2}{\rho} - \left(\frac{x_1 \cdot M_1}{\rho_1} + \frac{x_2 \cdot M_2}{\rho_2}\right) \quad (1)$$

where x_i, M_i, and ρ_i are respectively the mole fraction, molar mass, and density of component i in the mixture. Analogously, the change of isentropic compressibility by mixing ($\Delta\kappa_s$) and the change of molar refraction by mixing (ΔR), of thermodynamic interest, were calculated as:

$$\Delta\kappa_s = \kappa_s - \left(\phi_1 \cdot \kappa_{s,1} + \phi_2 \cdot \kappa_{s,2}\right) \quad (2)$$

$$\Delta R = R_M - \left(x_1 \cdot R_{M,1} + x_2 \cdot R_{M,2}\right) \quad (3)$$

where ϕ_i represents the volume fraction of component *i* in the mixture:

$$\phi_i = \frac{x_i \cdot V_i}{x_1 \cdot V_1 + x_2 \cdot V_2} \quad (4)$$

and the isentropic compressibility (κ_s) was calculated as:

$$\kappa_s = \frac{1}{u^2 \cdot \rho} \quad (5)$$

and the molar refraction (R_M) was obtained via the Lorentz-Lorenz equation:

$$R_M = \frac{n_D^2 - 1}{n_D^2 + 2} \cdot \frac{x_1 \cdot M_1 + x_2 \cdot M_2}{\rho} \quad (6)$$

The numerical values of V^E, $\Delta\kappa_s$, and ΔR thus calculated for the binary systems methanol + [C$_2$mim][SCN] and ethanol + [C$_2$mim][SCN] are also included in Table 2. For the binary systems methanol + [C$_2$mim][OAc] and ethanol + [C$_2$mim][OAc], the values of ρ, n_D, V^E, and ΔR at the same temperature and pressure, and over the entire composition ranges, were previously determined elsewhere [22, 23, 34].

Table 2. Density (ρ), speed of sound (u), refractive index (n_D), excess molar volume (V^E), change of isentropic compressibility by mixing ($\Delta\kappa_s$), and change of molar refraction by mixing (ΔR), at 298.15 K and atmospheric pressure, for the binary systems (methanol or ethanol) (1) + [C$_2$mim][SCN] (2).[a]

x_1	ρ / g·cm^{-3}	u / m·s^{-1}	n_D	V^E / cm^3·mol^{-1}	$\Delta\kappa_s$ / TPa^{-1}	ΔR / cm^3·mol^{-1}
Methanol (1) + [C$_2$mim][SCN] (2)						
0.0000	1.1151	1851	1.55065	0.000	0	0.000
0.1297	1.1052	1831	1.54281	-0.350	-30	0.027
0.2018	1.0985	1813	1.53843	-0.511	-42	0.057
0.3185	1.0862	1780	1.52943	-0.832	-66	0.080
0.4076	1.0735	1750	1.51995	-0.957	-86	0.094
0.5037	1.0570	1711	1.50836	-1.110	-112	0.101
0.5936	1.0374	1655	1.49377	-1.225	-136	0.100
0.6923	1.0091	1585	1.47381	-1.309	-167	0.090
0.8050	0.9626	1477	1.44104	-1.301	-201	0.072
0.9014	0.8993	1328	1.39839	-1.002	-190	0.052
1.0000	0.7868	1103	1.32660	0.000	0	0.000
Ethanol (1) + [C$_2$mim][SCN] (2)						
0.0000	1.1151	1851	1.55065	0.000	0	0.000
0.1175	1.1016	1826	1.54280	-0.368	-26	0.045
0.2134	1.0889	1797	1.53506	-0.650	-48	0.050
0.3450	1.0677	1751	1.52227	-0.975	-79	0.058
0.3836	1.0605	1729	1.51795	-1.061	-87	0.060
0.5009	1.0352	1667	1.50291	-1.287	-115	0.068
0.5142	1.0318	1662	1.50095	-1.295	-120	0.071
0.6181	1.0031	1592	1.48410	-1.443	-145	0.076
0.6948	0.9757	1524	1.46827	-1.380	-157	0.081
0.7997	0.9282	1412	1.44082	-1.148	-156	0.070
0.8944	0.8733	1285	1.40936	-0.900	-117	0.045

[a] Uncertainties: $u(x) = 0.0002$, $u(P) = 5$ kPa, $u(\rho) = 0.0001$ g/cm^3, $u(T_\rho) = 0.1$ K, $u(u) = 1$ m·s^{-1}, $u(T_u) = 0.1$ K, $u(n_D) = 0.00004$, $u(T_{nD}) = 0.02$ K.

Fig. 2 shows the evolution of ρ, u, n_D, V^E, $\Delta\kappa_s$, and ΔR with composition for the systems methanol + [C$_2$mim][SCN] and ethanol + [C$_2$mim][SCN] at 298.15 K and atmospheric pressure. The three physical properties (ρ, u, and n_D) decrease with increasing concentrations of the alcohol (methanol or ethanol) in the mixture. Regarding V^E, its values are negative over the entire composition range, with a minimum of ca. -1.3 cm^3/mol in the case of the system with methanol and ca. -1.4 cm^3/mol for the system with ethanol. This is similar to the case of the corresponding systems with [C$_2$mim][OAc], for which minima in the same range of values were previously reported [22, 23]. The high negative deviations from ideality in these systems are the result of strongly attractive intermolecular interactions of the ILs with the alcohols (electrostatic, dipole, and hydrogen bonding forces) and efficient molecular packing (occupation of the IL interstices by alcohol molecules). A more detailed analysis of the relative relevance of the different types of interactions is not possible from the experimental data reported herein, although a stronger relevance of hydrogen bonding may be presumed in the systems with [C$_2$mim][OAc] as a result of its quite strong hydrogen bond donating ability [35, 36]. The curves of $\Delta\kappa_s$ describe a similar trend to those of V^E. In contrast, the positive values of ΔR describe a trend that exhibits a maximum, for any of the studied systems.

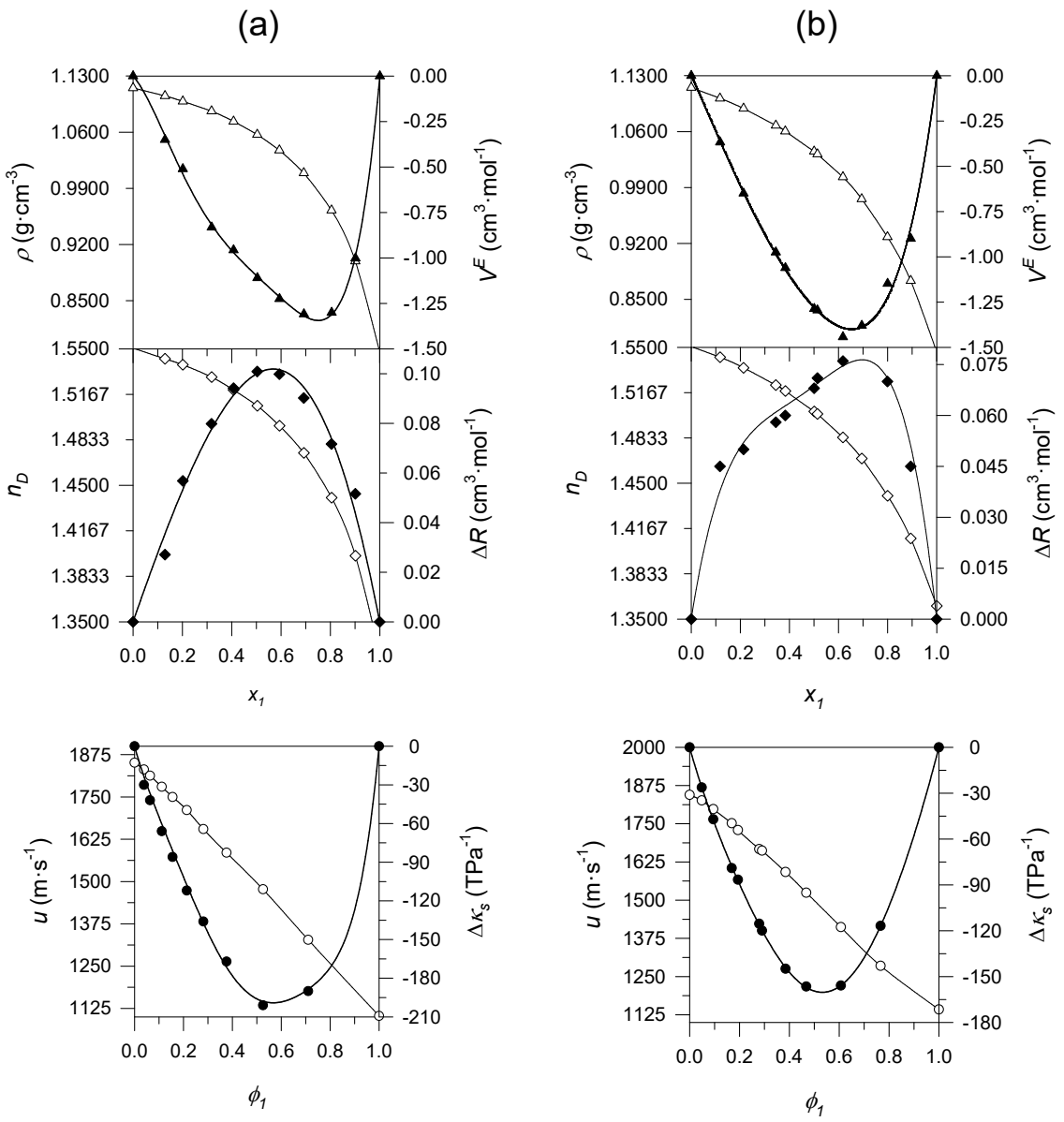

Fig. 2. Density (ρ, open triangles), refractive index (n_D, open diamonds), speed of sound (u, open circles), excess molar volume (V^E, solid triangles), change of molar refraction by mixing (ΔR, solid diamonds), and change of isentropic compressibility by mixing ($\Delta\kappa_s$), at 298.15 K and atmospheric pressure, for the systems (a) methanol + [C_2mim][SCN] and (b) ethanol + [C_2mim][SCN], as a function of the mole fraction of alcohol (x_1) or the volume fraction of alcohol (ϕ_1). Redlich-Kister polynomial fits are plotted as solid lines.

To obtain a mathematical description of V^E (or $\Delta\kappa_s$ or ΔR) with composition for its utilisation in precisely determining compositions in the compositional analysis of samples from the VLE experiments, the corresponding data were correlated for all four investigated systems by means of Redlich-Kister polynomials [37], that take the following form for binary mixtures:

$$Q = x_1 \cdot x_2 \cdot \sum_{k=0}^{m} [A_k \cdot (x_1 - x_2)^k] \quad (7)$$

where Q corresponds to the excess property or change of property by mixing to be correlated, x_1 and x_2 are the mole fractions of components *1* and *2* of the binary mixture, and k is a counter also serving as identifier of the m+1 polynomial coefficients A_k to be fit. These coefficients were obtained by least-squares regression applying Fisher's F-test to ascertain the statistical significance of the different terms and establish the value of m. The numerical values of the Redlich-Kister fit coefficients for the V^E of all four studied systems, along with the corresponding mean standard deviations, are listed in Table 3. The coefficients corresponding to the correlation of $\Delta\kappa_s$ and ΔR are listed in Table S2 in the Supplementary Material. The correlations are graphically depicted in Fig. 2, providing visual evidence of the satisfactory description of V^E, $\Delta\kappa_s$, and ΔR by the polynomial expansion of Redlich-Kister.

Table 3. Coefficients A_k of the Redlich-Kister polynomials, together with the corresponding standard deviations (σ), for the correlation of the excess molar volume V^E, expressed in $cm^3 \cdot mol^{-1}$, of the binary systems (methanol or ethanol) + [C_2mim][OAc] [22, 23] and (methanol or ethanol) + [C_2mim][SCN], at 298.15 K and atmospheric pressure.

System	A_0	A_1	A_2	A_3	σ
Methanol + [C_2mim][OAc]	-4.0927	3.0466	-3.4890	2.9549	0.013
Ethanol + [C_2mim][OAc]	-3.3014	2.0936	-2.2661	1.7622	0.013
Methanol + [C_2mim][SCN]	-4.3885	-2.5689	-3.8829	-4.1944	0.014
Ethanol + [C_2mim][SCN]	-5.1218	-2.8611	-1.6581	-0.9438	0.032

3.2. Vapour-liquid equilibrium

Table 4 lists the isobaric VLE data, at 101.25, 50, and 25 kPa, for the binary systems (methanol or ethanol) + [C_2mim][OAc], and Table 5 for (methanol or ethanol) + [C_2mim][SCN]. In particular, experimental values relating liquid composition and boiling temperature are reported for each specific pressure investigated. Since the IL is non-volatile, the vapour phase is exclusively constituted by alcohol. As it could be expected, an increase in the boiling (bubble) temperature is observed with a decrease of the mole fraction of alcohol in the liquid phase; or, equivalently, with an increase of the global composition of ionic liquid in the system. Compositions very rich in IL were not experimentally covered, due to the limited thermal stability of the ILs.

Table 4. Experimental isobaric vapour-liquid equilibrium data for the binary systems methanol + [C_2mim][OAc] and ethanol + [C_2mim][OAc] at 101.32, 50, and 25 kPa.[a]

P = 101.32 kPa		P = 50 kPa		P = 25 kPa	
T / K	x_1	T / K	x_1	T / K	x_1
Methanol (1) + [C_2mim][OAc] (2)					
338.53	0.9761	321.31	0.9869	306.45	0.9736
339.15	0.9644	321.68	0.9739	307.30	0.9585
339.72	0.9512	322.37	0.9599	308.39	0.9369
340.72	0.9368	323.61	0.9332	309.96	0.9122
342.74	0.9104	325.60	0.9080	311.73	0.8904
344.43	0.8904	328.10	0.8788	313.68	0.8665
347.21	0.8641	330.38	0.8555	315.22	0.8508
349.88	0.8423	333.46	0.8272	317.45	0.8314
353.90	0.8139	336.38	0.8064	319.29	0.8131
357.16	0.7907	340.18	0.7786	322.85	0.7883
361.04	0.7659	344.09	0.7520	325.64	0.7687
364.23	0.7490	354.06	0.6894	331.97	0.7249
368.76	0.7212	359.25	0.6580	334.81	0.7064
372.12	0.7005	364.55	0.6287	339.12	0.6808
375.07	0.6847	370.02	0.5934	343.56	0.6538
379.48	0.6631	375.02	0.5646	350.61	0.6071
383.79	0.6381	378.15	0.5344	354.96	0.5813
386.61	0.6191	383.50	0.5143	360.69	0.5490
390.21	0.5992	389.19	0.4846	366.76	0.5166
392.88	0.5793	393.89	0.4587	371.08	0.4795
397.01	0.5588	402.46	0.4062	375.29	0.4452
402.86	0.5147	406.18	0.3922	380.29	0.4192
408.22	0.4891	413.03	0.3351	388.81	0.3511
412.86	0.4592	423.23	0.2983		
417.75	0.4284	430.60	0.2616		
421.13	0.3965				
Ethanol (1) + [C_2mim][OAc] (2)					
351.63	0.9944	334.87	0.9908	320.11	0.9823
351.96	0.9840	336.81	0.9488	320.99	0.9578
352.32	0.9741	340.35	0.9170	323.38	0.9197
353.00	0.9592	342.72	0.9001	326.38	0.8838
354.20	0.9397	345.87	0.8766	328.59	0.8629
355.57	0.9218	348.99	0.8503	331.37	0.8362
357.47	0.9014	351.78	0.8258	334.37	0.8134
360.47	0.8731	354.75	0.8054	338.34	0.7842
362.28	0.8592	359.38	0.7534	341.55	0.7619
365.10	0.8388	363.01	0.7317	345.34	0.7352
366.28	0.8303	365.78	0.7121	349.03	0.7088
369.65	0.8061	369.80	0.6837	352.75	0.6808
373.44	0.7827	372.89	0.6633	359.00	0.6358
382.15	0.7293	374.99	0.6507	361.55	0.6160
387.33	0.6999	378.35	0.6244	363.79	0.6058
391.20	0.6788	380.49	0.6127	367.89	0.5703
396.75	0.6457	381.75	0.6003	370.89	0.5448
399.72	0.6261	383.44	0.5890	374.95	0.5141
406.45	0.5900	387.21	0.5632	378.56	0.4880

412.01	0.5291	389.49	0.5471	381.80	0.4597
412.01	0.5285	393.34	0.5190	384.65	0.4380
416.17	0.5016	395.74	0.5023	388.95	0.4109
423.42	0.4639	398.61	0.4823	391.91	0.3888
426.81	0.4265	402.16	0.4573	399.25	0.3354
		406.85	0.4317	401.25	0.3255
		412.72	0.4038	408.10	0.2885
		418.75	0.3782	417.27	0.2569
		423.00	0.3558	420.57	0.2374
		429.17	0.3290		

[a] Uncertainties: $u(T) = 0.1$ K, $u(P) = 0.005$ kPa, $u(x) = 0.001$.

Table 5. Experimental isobaric vapour-liquid equilibrium data for the binary systems methanol + [C_2mim][SCN] and ethanol + [C_2mim][SCN]) at 101.32, 50, and 25 kPa.[a]

P = 101.32 kPa		P = 50 kPa		P = 25 kPa	
T / K	x_1	T / K	x_1	T / K	x_1
Methanol (1) + [C_2mim][SCN] (2)					
338.09	0.9927	320.30	0.9931	308.39	0.8962
338.66	0.9749	320.58	0.9844	309.45	0.8606
339.31	0.9531	320.95	0.9694	311.95	0.7921
340.49	0.9196	321.33	0.9559	314.30	0.7411
341.56	0.8910	321.87	0.9375	316.75	0.6912
342.25	0.8737	322.33	0.9133	319.20	0.6475
343.38	0.8474	323.95	0.8907	322.75	0.5902
345.97	0.7965	324.73	0.8671	326.69	0.5320
347.21	0.7732	326.75	0.8132	330.94	0.4778
348.65	0.7471	330.09	0.7488	333.66	0.4455
352.13	0.6995	333.02	0.6992	337.58	0.4046
355.49	0.6433	336.55	0.6433	341.63	0.3644
357.13	0.6303	344.05	0.5461	346.65	0.3221
357.60	0.6251	349.97	0.4740	349.71	0.3035
358.64	0.6114	355.05	0.4347	355.48	0.2752
360.05	0.5968	358.68	0.4072	358.65	0.2546
360.82	0.5861	364.75	0.3572	362.85	0.2269
361.82	0.5729	368.15	0.3285	367.79	0.1968
363.01	0.5598	370.20	0.3126	380.10	0.1445
365.15	0.5377	377.49	0.2724		
367.01	0.5243	381.05	0.2568		
368.57	0.5099	386.51	0.2258		
372.80	0.4611	390.65	0.1989		
375.60	0.4490				
383.50	0.3974				
407.07	0.2199				
413.51	0.1957				
420.21	0.1725				
Ethanol (1) + [C_2mim][SCN] (2)					
351.91	0.9794	334.64	0.9993	319.73	0.9994
352.15	0.9687	335.14	0.9556	320.14	0.986
352.58	0.9512	335.46	0.9440	320.63	0.9596

352.79	0.9427	335.77	0.9265	320.98	0.9405
353.16	0.9259	336.25	0.8989	321.28	0.9211
353.42	0.9156	336.75	0.8685	322.04	0.8726
353.65	0.9060	337.59	0.8430	322.46	0.8479
354.09	0.8912	338.24	0.8223	323.42	0.8090
354.34	0.8822	339.02	0.8009	324.03	0.7822
355.10	0.8547	340.01	0.7680	324.60	0.7605
355.54	0.8375	341.24	0.7399	326.17	0.7103
355.81	0.8277	342.71	0.7056	328.45	0.6454
356.38	0.8145	344.32	0.6636	329.96	0.6081
356.96	0.7997	346.17	0.6198	331.33	0.5741
357.70	0.7807	347.27	0.5956	332.47	0.5556
358.85	0.7521	348.87	0.5589	333.66	0.5263
360.25	0.7175	354.27	0.4592	334.41	0.5137
364.35	0.6371	355.36	0.4442	336.71	0.4729
375.60	0.4650	357.43	0.4207	338.87	0.4391
380.28	0.4094	359.64	0.4000	342.65	0.3852
382.28	0.3900	368.27	0.3141	346.61	0.3355
391.85	0.3253	369.83	0.2949	348.53	0.3146
399.75	0.2548	371.13	0.2851	354.41	0.2778
408.05	0.2033	374.95	0.2591	357.60	0.2625
		376.48	0.2466	367.26	0.2063
		377.74	0.2359		
		379.49	0.2270		
		382.49	0.2231		
		389.38	0.1911		

[a] Uncertainties: $u(T) = 0.1$ K, $u(P) = 0.005$ kPa, $u(x) = 0.001$.

Temperature-composition diagrams are shown in Fig. 3 and Fig. 4 for all the systems studied. For each IL, and as it was expected, at a given pressure the equilibrium temperatures are lower for the system with methanol than for the system with ethanol. For each alcohol, at a given composition of the liquid phase, higher equilibrium temperatures were found with the IL [C_2mim][OAc], likely due to the stronger hydrogen bonding interactions caused by the acetate anion.

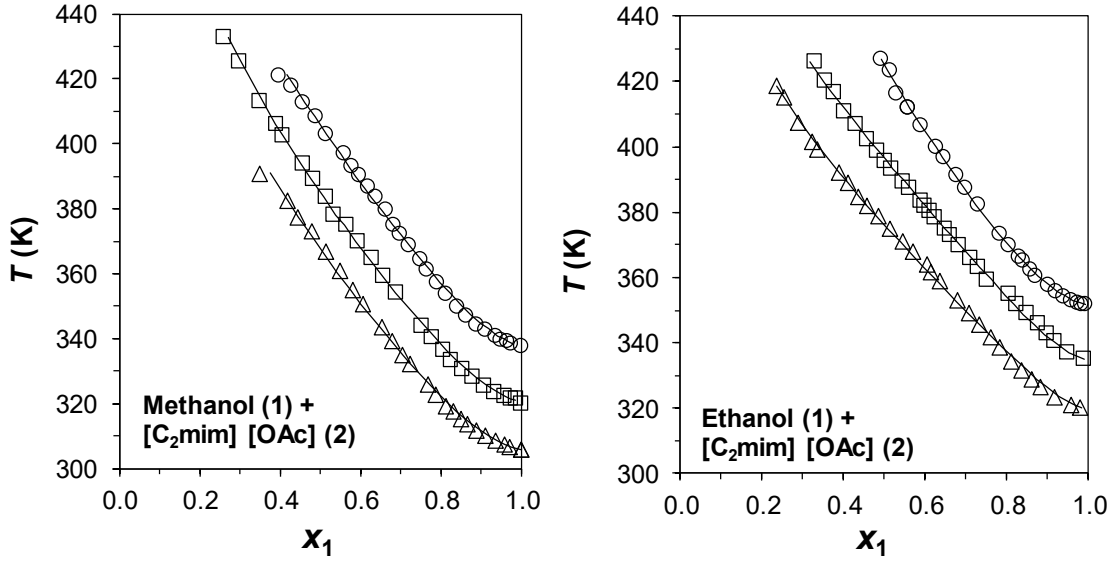

Fig. 3. Temperature-composition diagrams (liquid saturation lines) for the experimental VLE data of the binary systems (methanol or ethanol) + [C_2mim][OAc] at 101.32 kPa (○), 50 kPa (□), and 25 kPa (Δ), as a function of the mole fraction of alcohol (x_1). The vapour saturation lines are omitted, as they correspond to pure alcohol (x_1 = 1.0) in all cases. NRTL correlations are plotted as solid lines.

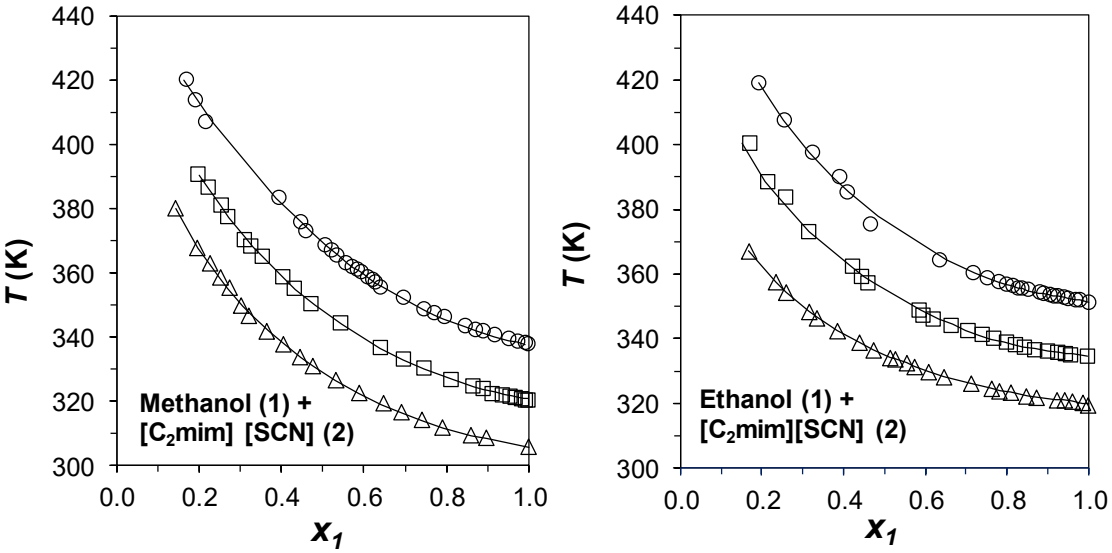

Fig. 4. Temperature-composition diagrams (liquid saturation lines) for the experimental VLE data of the binary systems (methanol or ethanol) + [C_2mim][SCN] at 101.32 kPa (○), 50 kPa (□), and 25 kPa (Δ), as a function of the mole fraction of alcohol (x_1). The vapour saturation lines are omitted, as they correspond to pure alcohol (x_1 = 1.0) in all cases. NRTL correlations are plotted as solid lines.

The correlation of the experimental VLE data (pressure, temperature, liquid mole fraction, and vapour mole fraction) was performed with a non-linear regression method based on the maximum likelihood principle. The vapour phase was considered ideal since

the IL can be considered totally non-volatile, and the alcohol is the only component in the vapour phase. Saturation pressures were calculated by means of Antoine's equation [38]. The corresponding coefficients for the alcohols were retrieved from the literature (see Table S3 in the Supplementary Material). For the ILs, the coefficients were arbitrarily set to fictional values leading to a negligible vapour pressure. The NRTL model was used to calculate the liquid phase activity coefficient, setting the non-randomness parameter α to different values (0.1, 0.2, and 0.3), and selecting the value giving the best correlation. Table 6 lists the model fit parameters for each system at each pressure, together with the standard deviation in temperature, pressure, and liquid and vapour compositions. The satisfactory quality of the NRTL correlations can be graphically assessed in Fig. 3 and Fig. 4, where they have been plotted along with the experimental VLE data. Nevertheless, in order to render the output of the simulation of the processes more reliable, a simultaneous correlation of all the data sets (all three pressures) for each system was also carried out. The results of these simultaneous correlations correspond to the rows labelled as "all" in the first column (pressure) in Table 6. As it can be observed, the resulting standard deviations are slightly higher, but still satisfactory.

Table 6. Binary interaction parameters (Δg_{12}, Δg_{21}) and standard deviations (σ) in temperature (T), liquid mole fraction (x), vapour mole fraction (y), and pressure (P), for the correlation of the VLE data with the NRTL model (using the indicated non-randomness parameter α), at each of the three investigated pressures, for the four binary systems studied in this work.

P / kPa	α	Δg_{12} / J·mol^{-1}	Δg_{21} / J·mol^{-1}	$\sigma(T)$ / K	$\sigma(x)$	$\sigma(y)$	$\sigma(P)$ / kPa
Methanol (1) + [C$_2$mim][OAc] (2)							
101.32	0.1	13114	-19828	0.14	0.0079	0.0002	0.011
50	0.1	7783.5	-17651	0.11	0.0064	0.0006	0.017
25	0.1	5927.2	-16858	0.12	0.0086	0.0007	0.039
all	0.1	7757.7	-17695	0.14	0.0075	0.0006	0.025
Ethanol (1) + [C$_2$mim][OAc] (2)							
101.32	0.1	4281.0	-17794	0.07	0.0037	0.0001	0.005
50	0.2	3912.1	-13105	0.12	0.0066	0.0006	0.011
25	0.2	3709.4	-12533	0.15	0.0069	0.0016	0.037
all	0.2	4231.8	-13006	0.18	0.0095	0.0010	0.035
Methanol (1) + [C$_2$mim][SCN] (2)							
101.32	0.1	-15967	23040	0.14	0.0045	0.0001	0.011
50	0.1	-14411	18068	0.23	0.0036	0.0009	0.031
30	0.1	-12407	14087	0.10	0.0037	0.0022	0.025
all	0.1	252.84	- 4325.3	0.26	0.0087	0.0001	0.049
Ethanol (1) + [C$_2$mim][SCN] (2)							
101.32	0.1	18587	-12688	0.04	0.0046	0.0004	0.001
50	0.1	11924	-7079.4	0.12	0.0068	0.0011	0.004
30	0.1	10974	-6465.6	0.02	0.0007	0.0018	0.051

all	0.2	11210	- 6906.6	0.12	0.0106	0.0012	0.223

3.3. Process simulation

For evaluation of the recovery of the IL ([C_2mim][OAc] or [C_2mim][SCN]) from its mixtures with alcohol (methanol or ethanol) at an industrial level, the simulation of the process scheme in Fig. 1 was performed with Aspen Plus, using the correlation of the experimental VLE data with the NRTL model. For the fixed feed of flowrate 100 kmol/h and IL mole fraction x_{IL} = 0.20 at 298.15 K and 101.32 kPa, the pressure and temperature in the flash unit were varied to analyse the composition of the liquid obtained and the energy requirements (calculated as the sum of the heat flow rates denoted as Q_H and Q_{HF} in Fig. 1). For subatmospheric pressures, the energy associated to a vacuum pump was not considered in the evaluation of these energy requirements. The results are shown in Fig. 5 and Fig. 6. It must be noted that simulations at pressures and temperatures outside the range of data obtained experimentally are extrapolations, and consequently the corresponding results should be taken with caution.

Methanol + [C_2mim][OAc]

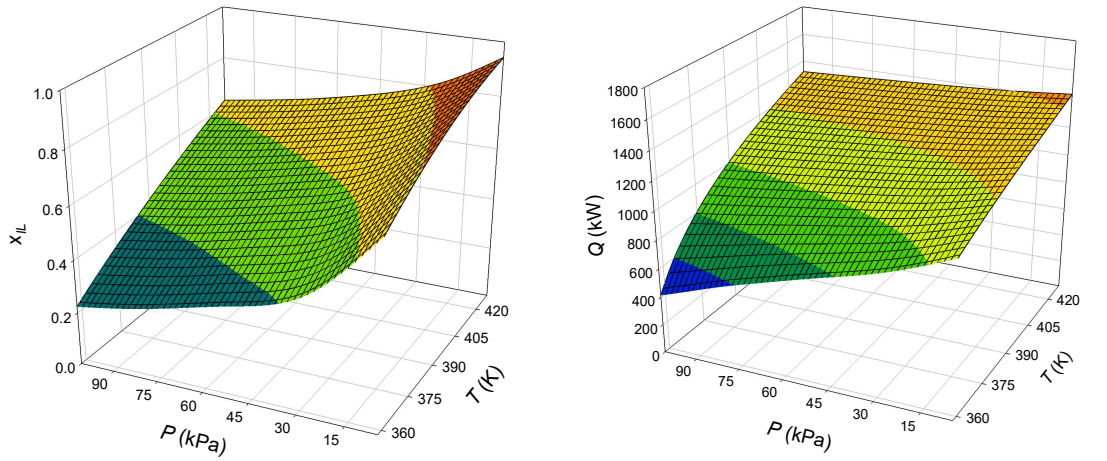

Ethanol + [C_2mim][OAc]

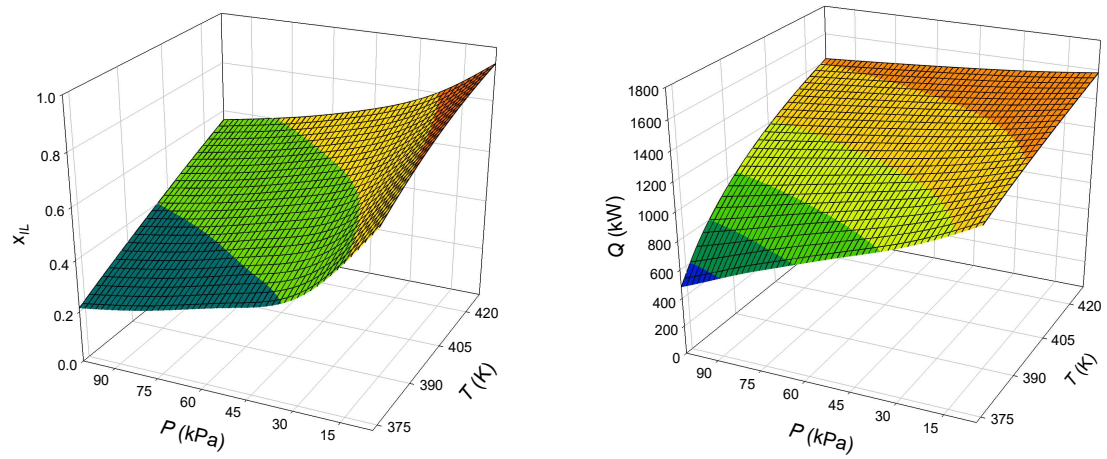

Fig. 5. IL mole fractions in the obtained IL-rich stream (x_{IL}), and required heat duties (Q), in a flash unit (Fig. 1) used for the regeneration of [C_2mim][OAc] from its mixture with methanol or ethanol, as a function of operating pressure (P) and temperature (T).

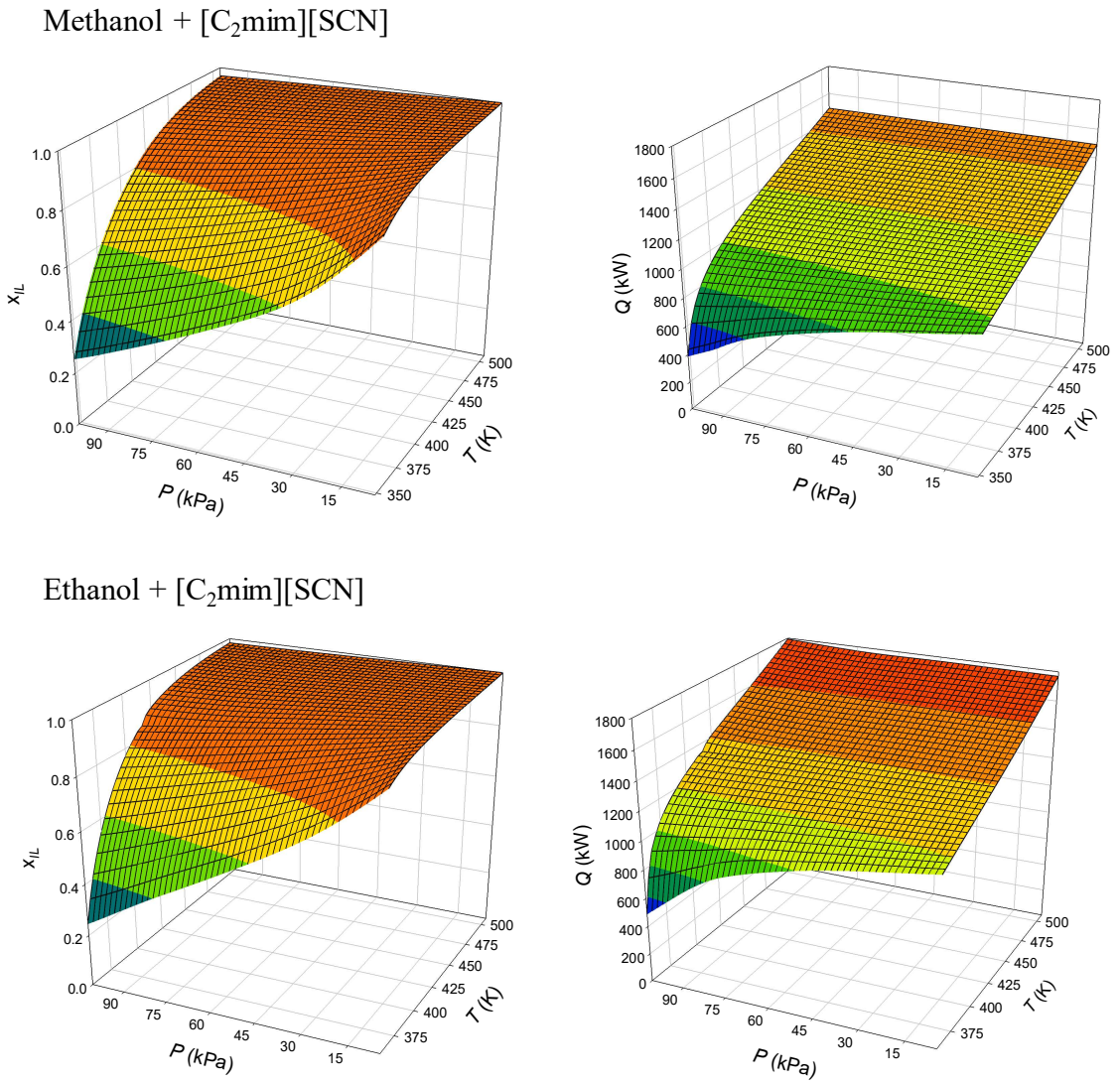

Fig. 6. IL mole fractions in the obtained IL-rich stream (x_{IL}), and required heat duties (Q), in a flash unit (Fig. 1) used for the regeneration of [C2mim][SCN] from its mixture with methanol or ethanol, as a function of operating pressure (P) and temperature (T).

In the case of the IL [C2mim][OAc] mixed with methanol, work pressures from 101.32 to 5 kPa at the maximum acceptable temperature of 423 K led to mole fractions of the recovered IL from 0.60 to 0.94, with the corresponding energy requirements ranging from ca. 1300 to ca. 1400 kW. The results in the case of the mixtures of this IL with ethanol led to lower recovered IL concentrations (IL mole fractions from 0.53 to 0.93) and somewhat higher energy requirements (from ca. 1400 to ca. 1550 kW). Thus, in none of these two cases the [C2mim][OAc] could be recovered as 'pure' IL, even if applying a level of vacuum as high as to work at an absolute pressure of 5 kPa. This was

also found by Kulajanpeng et al. [13] when they tried to recover the same IL after its use as entrainer in the extractive distillation of the water/ethanol system.

In contrast, for [C_2mim][SCN], IL compositions close to 0.98 could be obtained, working at 101.32 kPa without exceeding the decomposition temperature of the IL (513 K), for both the system with methanol and the system with ethanol. The same degree of purity in the recovered IL could be obtained, for instance, at temperatures of 468 and 473 K (with energy requirements of ca. 1350 and ca. 1600 kW) for the systems with methanol and with ethanol, respectively, if working at an absolute pressure of 25 kPa.

In the comparison of the results obtained for the systems with one and the other ionic liquid, it must be noted that a key aspect is the possibility of performing the flash distillation at a substantially higher temperature with [C_2mim][SCN] (up to 513 K) compared to [C_2mim][OAc] (up to 423 K). This clearly facilitates the best recovery performance of the unit for the systems involving [C_2mim][SCN].

It can be added that, in the practical application of the IL recovery process scheme, energy integration using the heat released to cool products ($Q_C + Q_{Cond}$ in Fig. 1) down to room temperature for the pre-heating of the feed stream could lead to significant savings in the energy required ($Q_H + Q_{HF}$).

4. Conclusions

The boiling (bubble) temperature of binary mixtures of the ILs [C_2mim][OAc] or [C_2mim][SCN] with the alcohols methanol or ethanol increases notoriously with an increase of the IL concentration in the mixture, as evidenced by the experimental determination of the isobaric VLE data for these binary systems at 101.32, 50, and 25 kPa. The experimental determination of this temperature at high concentrations of IL is precluded by the thermal stability of the IL itself. Of course, the vapour phase in equilibrium is constituted in all cases by pure alcohol. Novel data for the densities, speeds of sound, and refractive indices of the binary systems methanol + [C_2mim][SCN] and ethanol + [C_2mim][SCN] were complementary determined at 298.15 K and atmospheric pressure, with negative molar volumes being obtained with relatively high absolute values. This is indicative of the strong attractive forces existing between [C_2mim][SCN] and the alcohols, and is analogous to what had been previously observed for the case of the equivalent systems with [C_2mim][OAc] [22, 23].

In spite of the virtually infinite relative volatility of alcohols such as methanol or ethanol and ILs, the recovery of the ILs with high purity by distillation may not be necessarily achievable in an easy manner. According to simulations performed with Aspen Plus integrating the NRTL correlation of the experimental VLE data, this is the case of the recovery of [C_2mim][OAc]. For this IL, mole fractions lower than 0.95 were achieved when simulating its recovery in a flash unit, even operating at high vacuum (absolute pressure of 5 kPa) and at a temperature 423 K, nearly as high as possible taking into account the thermal stability reported for the IL. Conversely, in the case of [C_2mim][SCN], recovery from its mixtures with methanol or ethanol with a purity of ca. 0.98 in mole fraction was possible at atmospheric pressure or under more moderate vacuum levels (e.g. at an absolute pressure of 25 kPa, with energy requirements in the range 1350-1600 kW for operating temperatures in the range 468-473 K). Energy integration, for example via pre-heating of the feed with the hot streams exiting the flash unit, would significantly reduce the energy required in the separation process.

Acknowledgement

The authors acknowledge Xunta de Galicia for support through project ED431B 2017/023 and the Galician Network of Ionic Liquids (ED431D 2017/06) and the CRETUS Strategic Partnership (ED431E 2018/01), co-funded by the European Regional Development Fund. M.K.W. is grateful to the Erasmus + programme of the European Union for the award of a mobility traineeship.

Appendix A: Supplementary material

Supplementary data to this article can be found online at http://

References

[1] M. Freemantle, An Introduction to Ionic Liquids, RSC Publishing, Cambridge, 2010.

[2] W.L. Hough, M. Smiglak, H. Rodríguez, R.P. Swatloski, S.K. Spear, D.T. Daly, J. Pernak, J.E. Grisel, R.D. Carliss, M.D. Soutullo, J.H. Davis Jr., R.D. Rogers, The third evolution of ionic liquids: active pharmaceutical ingredients, New J. Chem. 31 (2007) 1429-1436.

[3] K.E. Gutowski, Industrial uses and applications of ionic liquids, Phys. Sci. Rev. 3 (2017) 20170191.

[4] J.F. Fernández, J. Neumann, J. Thöming, Regeneration, Recovery and Removal of Ionic Liquids, Curr. Org. Chem. 15 (2011) 1992-2014.

[5] P.M. Mathias, A. Soto, L. Fele-Zilnik, J.C. de Hemptinne, A. Bazyleva, J. Abildskov, Data quality and assessment, validation methods and error propagation through the simulation software, Chem. Eng. Res. Des. 137 (2018) A1-A8.

[6] M.T.G. Jongmans, J. Trampé, B. Schuur, A.B. de Haan, Solute recovery from ionic liquids: A conceptual design study for recovery of styrene monomer from [4-mebupy][BF_4], Chem. Eng. Proc. Int. 70 (2013) 148-161.

[7] V.R. Ferro, E. Ruiz, J. de Riva, J. Palomar, Introducing process simulation in ionic liquids design/selection for separation processes based on operational and economic criteria through the example of their regeneration, Sep. Purif. Technol. 97 (2012) 195-204.

[8] V.R. Ferro, J. de Riva, D. Sanchez, E. Ruiz, J. Palomar, Conceptual design of unit operations to separate aromatic hydrocarbons from naphtha using ionic liquids. COSMO-based process simulations with multi-component "real" mixture feed, Chem. Eng. Res. Des. 94 (2015) 632-647.

[9] P. Navarro, M. Larriba, J. García, F. Rodríguez, Design of the recovery section of the extracted aromatics in the separation of BTEX from naphtha feed to ethylene crackers using [4empy][Tf_2N] and [emim][DCA] mixed ionic liquids as solvent, Sep. Purif. Technol. 180 (2017) 149-156.

[10] M. Larriba, J. de Riva, P. Navarro, D. Moreno, N. Delgado-Mellado, J. García, V.R. Ferro, F. Rodríguez, J. Palomar, COSMO-based/Aspen Plus process simulation of the aromatic extraction from pyrolysis gasoline using the {[4empy][NTf2] + [emim][DCA]} ionic liquid mixture, Sep. Purif. Technol. 190 (2018) 211-227.

[11] I. Díaz, J. Palomar, M. Rodríguez, J. de Riva, V. Ferro, E.J. González, Ionic liquids as entrainers for the separation of aromatic-aliphatic hydrocarbon mixtures by extractive distillation, Chem. Eng. Res. Des. 115 (2016) 382-393.

[12] K. Weissermel, H.-J. Arpe, Industrial Organic Chemistry, 3rd ed., VCH, Weinheim, 1997.

[13] K. Kulajanpeng, U. Suriyapraphadilok, R. Gani, Systematic screening methodology and energy efficient design of ionic liquid-based separation processes, J. Clean. Prod. 111 (2016) 93-107.

[14] H.-H. Chen, M.-K. Chen, B.-C. Chen, I.-L. Chien, Critical Assessment of using an ionic liquid as entrainer via extractive distillation, Ind. Eng. Chem. Res. 56 (2017) 7768-7782.

[15] Z. Zhu, Y. Ri, H. Jia, X. Li, Y. Wang, Y. Wang, Process evaluation on the separation of ethyl acetate and ethanol using extractive distillation with ionic liquid, Sep. Purif. Technol. 181 (2017) 44-52.

[16] J. Cai, X. Cui, Y. Zhang, R. Li, T. Feng, Vapor-Liquid Equilibrium and Liquid-Liquid Equilibrium of Methyl Acetate + Methanol + 1-Ethyl-3-methylimidazolium Acetate, J. Chem. Eng. Data 56 (2011) 282-287.

[17] R. Li, X. Cui, Y. Zhang, T. Feng, J. Cai, Vapor-Liquid Equilibrium and Liquid-Liquid Equilibrium of Ethyl Acetate + Ethanol + 1-Ethyl-3-methylimidazolium Acetate, J. Chem. Eng. Data 57 (2012) 911-917.

[18] V. Dohnal, E. Baránková, A. Blahut, Separation of methyl acetate + methanol azeotropic mixture using ionic liquid entrainers. Chem. Eng. J. 237 (2014) 199-208.

[19] W. Li, X. Chen, H. Yin, L. Li, T. Zhang, Isobaric Vapor-Liquid Equilibrium for 2-Butanone + Ethanol System Containing Different Ionic Liquids at 101.3 kPa, J. Chem. Eng. Data 63 (2018) 380-388.

[20] P.D.A. Bastos, F.S. Oliveira, L.P.N. Rebelo, A.B. Pereiro, I.M. Marrucho, Separation of azeotropic mixtures using high ionicity ionic liquids based on 1-ethyl-3-methylimidazolium thiocyanate, Fluid Phase Equilibr. 389 (2015) 48-54.

[21] M.R. Mosallanejad, M.R. Khosravi-Nikou, A. Shariati, Separation of ethanol from n-decane-ethanol mixtures using imidazolium based ionic liquids, J. Chem. Thermodyn. 131 (2019) 471-477.

[22] M.C. Castro, H. Rodríguez, A. Arce, A. Soto, Mixtures of Ethanol and the Ionic Liquid 1-Ethyl–3-methylimidazolium Acetate for the Fractionated Solubility of Biopolymers of Lignocellulosic Biomass, Ind. Eng. Chem. Res. 53 (2014) 11850-11861.

[23] M.C. Castro, A. Arce, A. Soto, H. Rodríguez, Influence of Methanol on the Dissolution of Lignocellulose Biopolymers with the Ionic Liquid 1-Ethyl-3-methylimidazolium Acetate, Ind. Eng. Chem. Res. 54 (2015) 9605-9614.

[24] K.R. Seddon, A. Stark, M.J. Torres, Influence of chloride, water, and organic solvents on the physical properties of ionic liquids, Pure Appl. Chem. 72 (2000) 2275-2287.

[25] J.A. Riddick, W.B. Bunger, T. Sakano (Eds.), Organic Solvents, 4th ed., John Wiley, New York, 1986.

[26] Q. Zhang, S. Cai, W. Zhang, Y. Lan, X. Zhang, Density, viscosity, conductivity, refractive index and interaction study of binary mixtures of the ionic liquid 1-ethyl-3-methylimidazolium acetate with methyldiethanolamine, J. Mol. Liq. 233 (2017) 471-478.

[27] C.M.S.S. Neves, K.A. Kurnia, J.A.P. Coutinho, I.M. Marrucho, J.N. Canongia Lopes, M.G. Freire, L.P.N. Rebelo, Systematic Study of the Thermophysical Properties of Imidazolium-Based Ionic Liquids with Cyano-Functionalized Anions, J. Phys. Chem. B 117 (2013) 10271-10283.

[28] J.O. Valderrama, W.W. Sanga, J.A. Lazzús, Critical Properties, Normal Boiling Temperature, and Acentric Factor of Another 200 Ionic Liquids, Ind. Eng. Chem. Res. 47 (2008) 1318-1330.

[29] C. Su, X. Liu, C. Zhu, M. He, Isobaric molar heat capacities of 1-ethyl-3-methylimidazolium acetate and 1-hexyl-3-methylimidazolium acetate up to 16 MPa, Fluid Phase Equilibr. 427 (2016) 187-193.

[30] E. Zorebski, M. Musiał, K. Bałuszyńska, M.Zorębski, M. Dzida, Isobaric and Isochoric Heat Capacities as Well as Isentropic and Isothermal Compressibilities of Di- and Trisubstituted Imidazolium-Based Ionic Liquids as a Function of Temperature, Ind. Eng. Chem. Res. 57 (2018) 5161-5172.

[31] H. Renon, J.M. Prausnitz, Local Compositions in Thermodynamic Excess Functions for Liquid Mixtures, AIChE J. 14 (1968) 135-144.

[32] Y. Cao, T. Mu, Comprehensive Investigation on the Thermal Stability of 66 Ionic Liquids by Thermogravimetric Analysis, Ind. Eng. Chem. Res. 53 (2014) 8651-8664.

[33] P. Navarro, M. Larriba, E. Rojo, J. García, F. Rodríguez, Thermal Properties of Cyano-Based Ionic Liquids, J. Chem. Eng. Data 58 (2013) 2187-2193.

[34] M.C. Castro, PhD thesis, University of Santiago de Compostela, 2018.

[35] S. Zhang, X. Qi, X. Ma, L. Lu, Y. Deng, Hydroxyl Ionic Liquids: The Differentiating Effect of Hydroxyl on Polarity due to Ionic Hydrogen Bonds between Hydroxyl and Anions, J. Phys. Chem. B 114, 3912-3920.

[36] L.K.J. Hauru, M. Hummel, A.W.T. King, I. Kilpeläinen, H. Sixta, Role of solvent Parameters in the Regeneration of Cellulose from Ionic Liquid Solutions, Biomacromol. 13 (2012) 2896-2905.

[37] O. Redlich, A.T. Kister, Thermodynamics of Nonelectrolyte Solutions. Algebraic Representation of Thermodynamic Properties and the Classification of Solutions, Ind. Eng. Chem. 40 (1948) 345-348.

[38] I.M. Smallwood, Handbook of Organic Solvent Properties, Butterworth-Heinemann, London, 1996.